ERDC/CHL CETN-IV-25
June 2000

US Army Corps
of Engineers®

Enhancements of the Numerical Model of the Longshore Current NMLONG to Include Interaction Between Currents and Waves (NMLong-CW)

by Magnus Larson and Nicholas C. Kraus

PURPOSE: The Coastal Engineering Technical Note (CETN) herein describes the Numerical Model of the Longshore current for Current and Waves (NMLong-CW) that accounts for the interaction between a current and surface waves. NMLong-CW can simulate wave transformation, the steady-state wave-generated longshore current, and change in water level at an inlet by waves and wind. The interaction between a current and waves can significantly alter the wave height and wavelength. NMLong-CW is a one-dimensional model and is limited to situations were longshore uniformity applies.

BACKGROUND: The original numerical model NMLONG (Kraus and Larson 1991; Larson and Kraus 1991) was developed under the U.S. Army Corps of Engineers' Dredging Research Program. It calculates nearshore wave transformation, water level change, and longshore current across a single profile line, under the assumption of longshore uniformity in the profile and hydrodynamic processes. NMLONG solves the wave energy flux conservation equation, accounting for wave shoaling, refraction, breaking, and reforming. The transformation of random waves is calculated by Monte-Carlo simulation. Wave energy dissipation accompanying depth-limited breaking is described in accordance with Dally, Dean, and Dalrymple (1985). The cross-shore momentum equation is solved numerically to obtain the change in water level, and the equation governing alongshore momentum gives the distribution of the steady (time average on a wave scale) longshore current velocity across the shore. The longshore current and change in water level (setup and setdown) driven by a local wind can also be simulated. Nonlinear bottom friction is computed from an efficient approximation, and lateral mixing is modeled with an eddy viscosity that depends on the local wave orbital velocity and wave height.

Both tidal and wind-generated currents can be comparable to or exceed the strength of the wave-generated longshore current. Currents produced independently of waves as by wind and the tide may be in opposite directions, producing complex distributions of the current across the shore. The capability of representing the action of currents in NMLONG and the interaction between the current and waves resulted in a substantially revised model and name as NMLong-CW, where CW stands for interaction between currents and waves. In the revised model, wave transformation in the presence of a current is calculated from conservation of wave action flux instead of wave energy flux, and the wave dispersion relationship is modified to include a current.

NMLong-CW was revised to describe both depth- and steepness-limited wave breaking, and a unified formulation to quantify energy dissipation produced by these two types of breaking is employed. As before, the longshore current and mean water level are calculated through the alongshore and cross-shore momentum equations, respectively. However, in the alongshore

Report Documentation Page

Form Approved
OMB No. 0704-0188

1. REPORT DATE	2. REPORT TYPE	3. DATES COVERED
JUN 2000	**N/A**	**-**

4. TITLE AND SUBTITLE
Enhancements of the Numerical Model of the Longshore Current NMLONG to Include Interaction Between Currents and Waves (NMLong-CW)

5a. CONTRACT NUMBER

5b. GRANT NUMBER

5c. PROGRAM ELEMENT NUMBER

6. AUTHOR(S)
Larson, Magnus, and Kraus, Nicholas

5d. PROJECT NUMBER

5e. TASK NUMBER

5f. WORK UNIT NUMBER

7. PERFORMING ORGANIZATION NAME(S) AND ADDRESS(ES)
US Army Corps of Engineers, Engineer Research and Development Center, Coastal and Hydraulics Laboratory, Vicksburg, MS

8. PERFORMING ORGANIZATION REPORT NUMBER

9. SPONSORING/MONITORING AGENCY NAME(S) AND ADDRESS(ES)

10. SPONSOR/MONITOR'S ACRONYM(S)

11. SPONSOR/MONITOR'S REPORT NUMBER(S)

12. DISTRIBUTION/AVAILABILITY STATEMENT
Approved for public release, distribution unlimited

13. SUPPLEMENTARY NOTES
The original document contains color images.

14. ABSTRACT
This Coastal Engineering Technical Note (CETN) describes the Numerical Model of the Longshore current for Current and Waves (NMLong-CW) that accounts for the interaction between a current and surface waves. NMLong-CW can simulate wave transformation, the steady-state wave-generated longshore current, and change in water level at an inlet by waves and wind. The interaction between a current and waves can significantly alter the wave height and wavelength. NMLong-CW is a one-dimensional model and is limited to situations were longshore uniformity applies.

15. SUBJECT TERMS

16. SECURITY CLASSIFICATION OF:			17. LIMITATION OF ABSTRACT	18. NUMBER OF PAGES	19a. NAME OF RESPONSIBLE PERSON
a. REPORT	b. ABSTRACT	c. THIS PAGE			
unclassified	**unclassified**	**unclassified**	**UU**	**13**	

Standard Form 298 (Rev. 8-98)
Prescribed by ANSI Std Z39-18

momentum equation, provision for an external (large-scale) current has been incorporated in addition to the wave- and wind-driven currents. At present, the external current must be specified as an input, although in the future an option will be added allowing the user to generate current distributions within NMLong-CW corresponding to, for example, large-scale tidal currents and ebb jet flows. Additional background information on the current-and-wave interaction can be found in other CETNs (Smith 1997, 1999) produced under the Coastal Inlets Research Program (CIRP).

In the following, a summary is given of the equations used in NMLong-CW with focus on the enhancements made. The procedures for calculating wave transformation, longshore current, and water level change are discussed separately. Also, a section is included on wave blocking and the criterion applied to describe this phenomenon. Capabilities of NMLong-CW are demonstrated by examples. The model is operated through a graphical interface that runs on the Windows 95/98 and NT platforms for personal computers. NMLong-CW is at the state of the art in calculation of nearshore waves and currents, and this CETN documents the underlying physics implemented.

WAVE TRANSFORMATION: Under the condition of alongshore uniformity, wave transformation across a nearshore profile is described by the equation for conservation of wave action flux (e.g., Jonsson 1990):

$$\frac{d}{dx}\left(\frac{EC_{ga}\cos\beta}{\omega_r}\right)=\frac{E_D}{\omega_r} \tag{1}$$

where E is the wave energy (linear theory used), C_{ga} the absolute wave group speed, β the wave ray direction, ω_r the relative wave frequency (= $2\pi/T_r$, where T_r is the relative wave period), E_D the wave energy dissipation, and x the cross-shore axis pointing offshore. The presence of a current with magnitude U and direction δ will alter the wave transformation, and the expressions for C_{ga} and β may be obtained from geometric considerations to yield (see Figure 1 for a definition sketch):

$$C_{ga}=\left(C_{gr}^2+U^2+2C_{gr}U\cos(\delta-\alpha)\right)^{1/2} \tag{2}$$

$$\beta=\alpha+\arctan\left(\frac{U\sin(\delta-\alpha)}{U\cos(\delta-\alpha)+C_{gr}}\right) \tag{3}$$

where C_{gr} is the relative group speed, and α the direction of the wave orthogonal. The definitions of the angles are $-90 \le \alpha \le 90$ and $-180 \le \delta \le 180$.

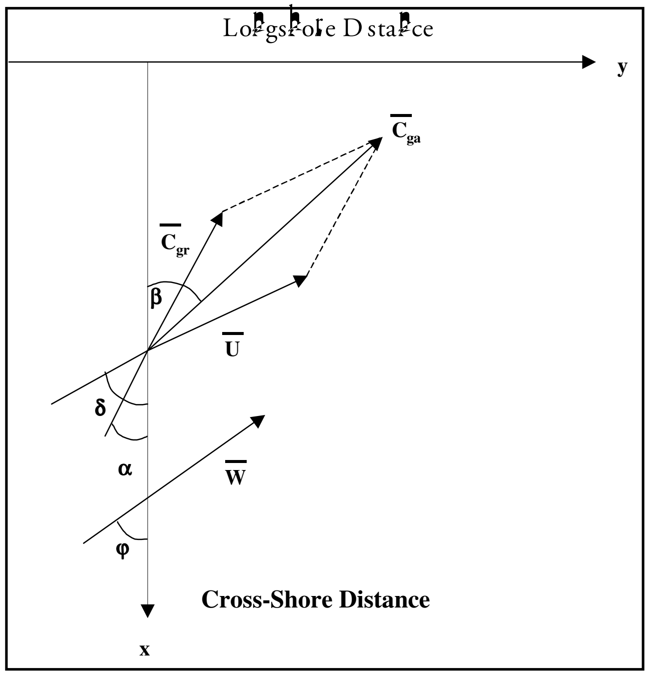

Figure 1. Definition sketch for waves propagating on a current (overbar implies a vector)

To determine the wave properties at a certain total depth $d = h + \eta$, where h is the still-water depth, and η is the mean deviation from still-water level (set up or set down), the dispersion relationship including a current has to be solved (Jonsson, Skougaard, and Wang 1970):

$$\sqrt{\frac{d}{L}\tanh kd} = \sqrt{\frac{d}{L_o}}\left(1 - \frac{U\cos(\delta-\alpha)T_a}{d}\frac{d}{L}\right) \tag{4}$$

in which T_a is the absolute wave period, L the wavelength at depth d, k the wave number ($2\pi/L$),and L_o denotes the deepwater wavelength neglecting the current ($=gT_a^2/2\pi$). Equation 4 is solved by a Newton-Raphson technique, which gives rapid convergence. The relative group speed is determined from:

$$C_{gr} = \frac{1}{2}C_r\left(1 + \frac{2kd}{\sinh 2kd}\right) \tag{5}$$

and the relative phase speed C_r is computed as:

$$C_r = \left(\frac{g}{k}\tanh kd\right)^{1/2} \tag{6}$$

in which g is the acceleration of gravity. As can be seen from Equation 4, the wave angle α must be known before the wave properties can be calculated. Thus, Snell's law is employed to

determine wave refraction and the variation in α across the profile. For a wave traveling between locations denoted by indices 1 and 2, Snell's law is written:

$$\frac{\sin\alpha_1}{L_1} = \frac{\sin\alpha_2}{L_2} \tag{7}$$

Equations 4 and 7 must be solved simultaneously because both α and L are unknown at the next grid point in the numerical calculations.

The wave energy dissipation in Equation 1 is given by (compare Smith, Resio, and Vincent 1997):

$$E_D = \frac{\kappa}{d_D}(E - E_s)C_{gr} \tag{8}$$

where κ is an empirical coefficient (= 0.15), d_D the length scale controlling the dissipation (equal to the water depth d in Dally, Dean, and Dalrymple (1985)), and E_s the energy of a stable wave for which breaking ceases and a wave can reform. To generalize Equation 8 to describe all water depths and both depth- and steepness-limited breaking, the following expressions are employed for the stable wave energy and the dissipation length scale:

$$E_s = \frac{1}{8}\rho g H_s^2 \tag{9}$$

$$H_s = \frac{\Gamma}{\gamma_b} H_b \tag{10}$$

$$d_D = \frac{H_b}{\gamma_b} \tag{11}$$

where ρ is the density of water, Γ is an empirical coefficient (= 0.4), and γ_b is the ratio between wave height and water depth at incipient breaking under depth-limiting conditions (typically taken to be 0.78). The wave height at incipient breaking is calculated from the Miche criterion, modified by Battjes and Janssen (1978) to be applicable for all water depths:

$$H_b = \frac{0.88}{k}\tanh\left(\frac{\gamma_b kd}{0.88}\right) \tag{12}$$

In shallow water, Equation 12 reduces to $H_b = \gamma_b d$, indicating that Equations 8-11 recover the original formulation by Dally, Dean, and Dalrymple (1985). Equation 12 is applied with the local water depth to determine H_b from which H_s is obtained from Equation 10.

WAVE BLOCKING: Waves propagating on a current may experience blocking, if the current is sufficiently strong and has a component opposing the waves. If blocking occurs, the wave

energy cannot be transported against the current, and the waves are "stopped" (in the real case this often implies confused wave conditions that could cause navigational hazards). The criterion for determining the limit for wave blocking is given by (Jonsson, Skougaard, and Wang 1970):

$$C_{gr} + U\cos(\delta - \alpha) = 0 \tag{13}$$

If Equation 13 is fulfilled, the denominator in Equation 9 becomes 0 and the wave rays (along which the energy is conserved) are perpendicular to the wave orthogonals. At the point of blocking, the wavelength attains its minimum value, which may be estimated from:

$$\sqrt{\frac{d}{L}\tanh kd} = \frac{1}{1-n}\sqrt{\frac{d}{L_o}} \tag{14}$$

where

$$n = \frac{1}{2}\left(1 + \frac{2kd}{\sinh 2kd}\right) \tag{15}$$

The required blocking speed associated with Equation 14 may be estimated from Equation 13, once the wavelength L at blocking has been determined for a specific L_o and d. This criterion may be written in non-dimensional form as:

$$\frac{U\cos(\delta - \alpha)}{gT_a} = -\frac{n}{2\pi}\sqrt{\frac{L}{d}\frac{d}{L_o}\tanh kd} \tag{16}$$

Thus, for a specific ratio d/L_o the required blocking speed might be determined from Equations 14 and 16. Figure 2 displays the non-dimensional blocking speed as a function of d/L_o.

Asymptotic solutions to the conditions for blocking may be readily obtained for shallow and deep water. In deep water, that is, $kd \to \infty$, Equation 14 yields:

$$L = \frac{1}{4}L_o \tag{17}$$

and Equation 16 produces:

$$U\cos(\delta - \alpha) = -\frac{1}{4}C_o \tag{18}$$

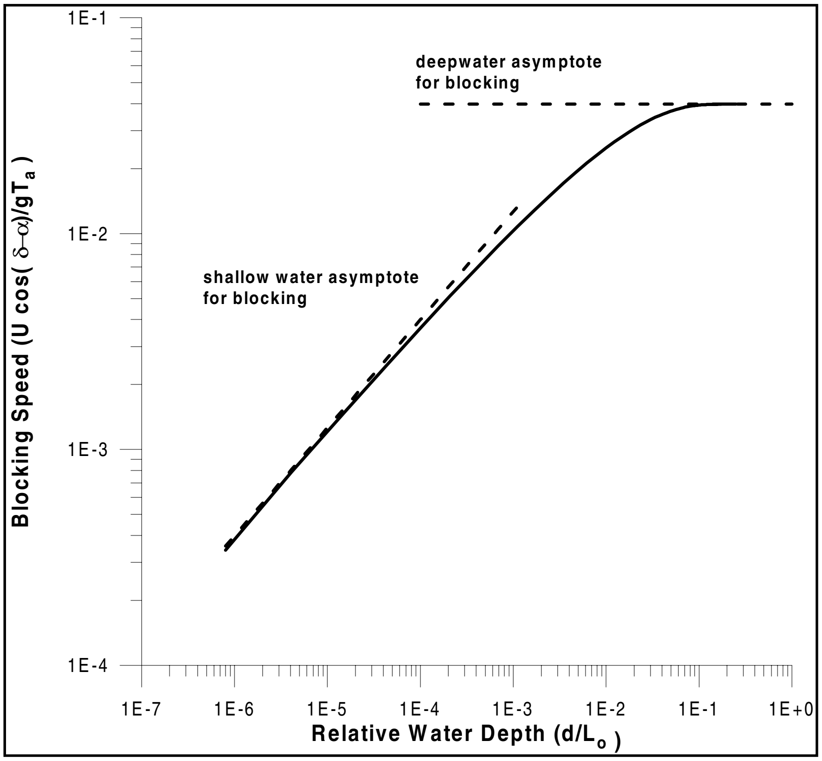

Figure 2. Non-dimensional blocking speed as a function of relative water depth

where C_o is the phase speed in deep water neglecting the current ($=gT_a/2\pi$). In shallow water, kd becomes small; omitting terms of order $(kd)^2$ and higher results in the following expression for the wavelength at blocking:

$$\frac{d}{L} = \left(\frac{9}{32\pi^5} \frac{d}{L_o} \right)^{1/6} \tag{19}$$

The corresponding current speed at blocking is given by:

$$\frac{U \cos(\delta - \alpha)}{gT_a} = -\frac{1}{\sqrt{2\pi}} \left(\frac{d}{L_o} \right)^{1/2} \tag{20}$$

This relationship is in fact identical to $U \cos(\delta\text{-}\alpha)=(gd)^{1/2}$. The asymptotes for deep and shallow water are indicated in Figure 2.

The wave equations are numerically solved by a finite-difference formulation similar to that in NMLONG. For representing waves with random height, a Monte-Carlo simulation is carried out for a large number of individual waves belonging to the Rayleigh probability density distribution in the offshore so that statistically stable wave quantities are obtained in averaging the results from all the waves. The Rayleigh distribution will not necessarily be followed as the waves propagate onshore and break or are modified by the current-wave interaction. Because the wave

transformation depends on the current field, the wave calculations are updated after the current has been computed (described next). This iteration between the wave and the current field is continued until convergence is achieved.

LONGSHORE CURRENT: After the wave transformation calculations, the longshore current is computed using the alongshore momentum equation where lateral mixing, bottom friction, and external forcing are included:

$$\frac{d}{dx}\left(\varepsilon d \frac{dV}{dx}\right) - f_{by} = \frac{1}{\rho}\frac{dS_{xy}}{dx} - R_w - R_{lc} \tag{21}$$

where V is the longshore current velocity, f_{by} the bottom friction stress (discussed later), ε a lateral mixing coefficient [(=$\Lambda H u_m$, where H is the wave height, for random waves taken to be the root-mean-square (rms) wave height, u_m the bottom orbital velocity, and Λ an empirical coefficient typically in the range 0.2-0.5), S_{xy} the radiation stress transported onshore and directed alongshore, and R_w and R_{lc} forcing associated with wind and an external (large-scale) current (e.g., tide), respectively. The velocity V constitutes the alongshore component of U; that is, $U=(V^2+U_c^2)^{1/2}$, where U_c is the mean cross-shore velocity (thus, the angle δ is given by $\tan^{-1}(V/U_c)$].

The forcing associated with a local wind is determined by:

$$R_w = C_D \frac{\rho_a}{\rho} |W| W \sin\varphi \tag{22}$$

where C_D is a drag coefficient given by the expression developed by the WAMDI Group (1988), ρ_a the air density, W the wind speed, and φ the wind direction (W and φ are defined in the same way as the current; see Figure 1). In NMLong-CW, it is possible to specify an external current, assumed to be associated with a large-scale circulation, such as the tide or a regional coastal current. To represent this current in the model, the forcing is derived from a term introduced as:

$$R_{lc} = c_f |U_{lc}| U_{lc} \tag{23}$$

where c_f is the bottom friction coefficient appearing in f_{by} (typically in the range 0.002-0.008 for field conditions), and U_{lc} the specified longshore component of the external current (the cross-shore component of this current is equal to U_c). The bottom friction stress f_{by} is calculated with Nishimura's square-wave approximation (Nishimura 1988) as described by Kraus and Larson (1991) to save substantial execution time yet incorporate the non-linear term.

Finally, the radiation stress S_{xy} is calculated from:

$$S_{xy} = \frac{1}{16}\rho g H^2 \frac{C_{gr}}{C_r} \sin 2\alpha \tag{24}$$

MEAN WATER LEVEL: The mean water level η (setup and setdown) is determined from the cross-shore momentum equation:

$$\rho g d \frac{d\eta}{dx} = -\frac{dS_{xx}}{dx} - C_D \rho_a \left|W\right| W \cos\varphi \tag{25}$$

in which S_{xx} is the radiation stress component transported and directed onshore, given by:

$$S_{xx} = \frac{1}{8}\rho g H^2 \left(\frac{C_{gr}}{C_r}(\cos^2\alpha + 1) - \frac{1}{2} \right) \tag{26}$$

For random waves, S_{xx} and S_{xy} are determined as averages for the selected number of waves in the Monte-Carlo simulation before they are inserted in the momentum equations. The cross-shore mean current does not enter Equation 25 and is assumed only to modify the wave transformation.

EXAMPLES:

Example 1: Wave transformation at an inlet entrance. Smith *et al*. (1998) measured wave breaking on a current at an idealized inlet in the laboratory. A 1:50 scale model of an inlet was constructed in a 46-m-wide by 99-m-long concrete basin with 0.6-m-high walls. The parallel jetties at the inlet had a spacing of 3.66 m and extended 5.5 m offshore. A seaward flowing (ebb) current U_c was generated between the jetties that diffused as it propagated offshore. The experimental conditions constituted permutations of the following parameter values: mean spectral wave height in deep water H_{mo} = 3.7 and 5.5 cm, spectral peak period T_p = 0.7 and 1.4 sec, wave direction perpendicular to the jetties, and U_c = 0, 12, and 24 cm/sec. Wave height and current were measured at several gauges around the inlet with the main objectives to study wave breaking and determining the decay in wave height on the current.

Here, two cases are discussed to illustrate the performance of NMLong-CW, in particular for the algorithm developed to calculate wave breaking on a current. These simulations were partly carried out to validate the generalization of Equation 8 (calculation of the energy dissipation on a current). It was found that the standard value of $\Gamma = 0.4$ overall provided reasonable results, although this value should be confirmed by further simulations against other data sets. The cases discussed here encompassed Case 5 (H_{mo} = 4.1 cm, T_p = 1.4 sec, U_c = 13 cm/sec) and Case 11 (H_{mo} = 3.9 cm, T_p = 0.83 sec, U_c = 24 cm/sec) from Smith *et al*. (1998) illustrating the results for both the weaker and stronger current cases. Wave height transformation was calculated by Monte-Carlo simulation with a Rayleigh distribution specified in the offshore. The actual simulated time series of waves at each location was input in the present cases to compute the significant wave height, which was assumed to be equal to H_{mo}. Figures 3a and 3b display the calculated significant wave height for Cases 5 and 11, respectively, together with the measured wave heights. Viewing Figure 3 together with other cases not shown here, the agreement between calculations and measurements is regarded as satisfactory.

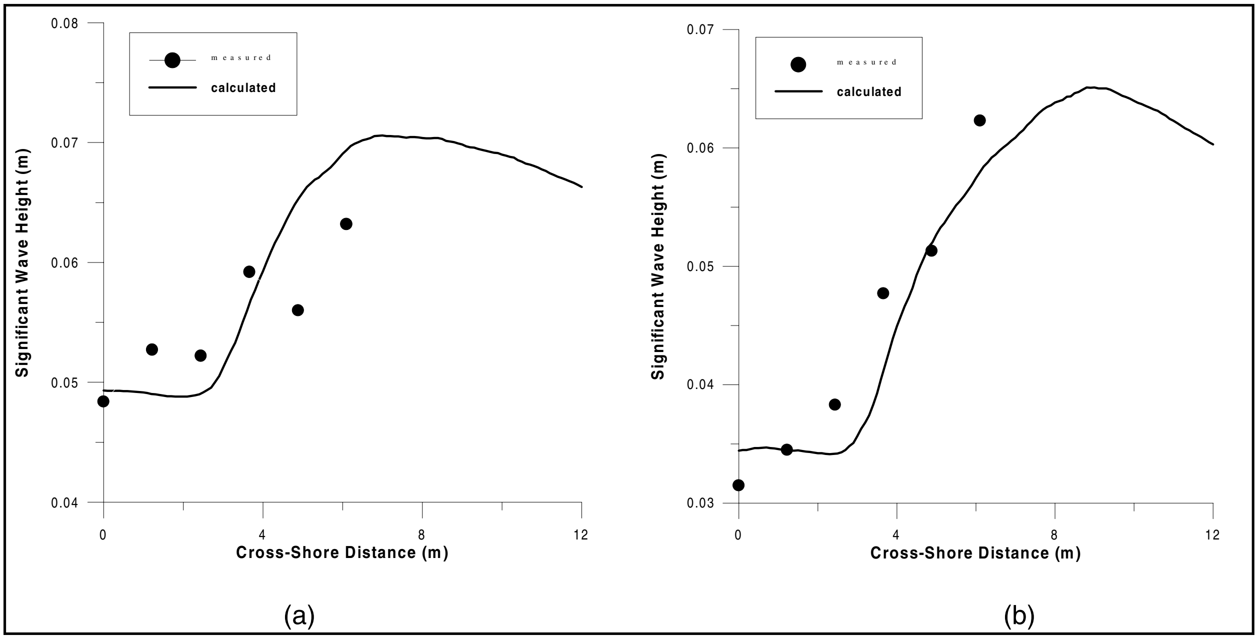

Figure 3. Comparison between calculated and measured significant wave height for Smith *et al*. (1998) (a) Case 5 and (b) Case 11

Example 2: Wave-generated longshore current in the presence of a large-scale current. To illustrate the capability in NMLong-CW to simulate the presence of a large-scale current and the wave-generated longshore current in the nearshore, a hypothetical example is discussed. An equilibrium profile shape in accordance with Dean (1977) was assumed with a shape parameter of $A = 0.1$ m$^{1/3}$ corresponding to a median sand grain size of about 0.2 mm. A root-mean-square (rms) wave height in deep water of $H_{rmso} = 2.0$ m with a mean period of $T = 8.0$ sec and a mean incident angle $\alpha_o = 30$ deg was specified (waves Rayleigh distributed in deep water). Also, a large-scale current was specified with an alongshore component growing exponentially from 0 at the shoreline to 0.5 m/sec in the offshore and having no component across shore ($\delta = 90$ deg). Standard (default) values were specified for the wave and longshore current parameters: $\gamma_b = 0.78$, $\kappa = 0.15$, $\Gamma = 0.4$, $\Lambda = 0.3$, and $c_f = 0.003$.

Figure 4 illustrates the simulated longshore current for waves and large-scale (L-S) current together as well as for waves only. Also, the cross-shore distribution of the input L-S current is shown in the figure. In the absence of waves, NMLong-CW exactly reproduces the input L-S current. However, if waves are present, the bottom friction stress will increase, and the simulated current will typically also differ from the L-S current outside the region of wave-generated currents. Because the influence of the waves disappears in deeper water, the simulated current will approach the input L-S current (if there is no wind-induced current).

Example 3: Wave transformation at an inlet in the presence of a flood and ebb current. This example involves inlet currents and waves representative of hydrodynamic conditions as observed at Shinnecock Inlet, Long Island, NY. For this example, NMLong-CW is operated to obtain information exclusively on cross-shore processes. It is cautioned that inlet entrances are complex and that results obtained from simplified calculation conditions should be interpreted with caution.

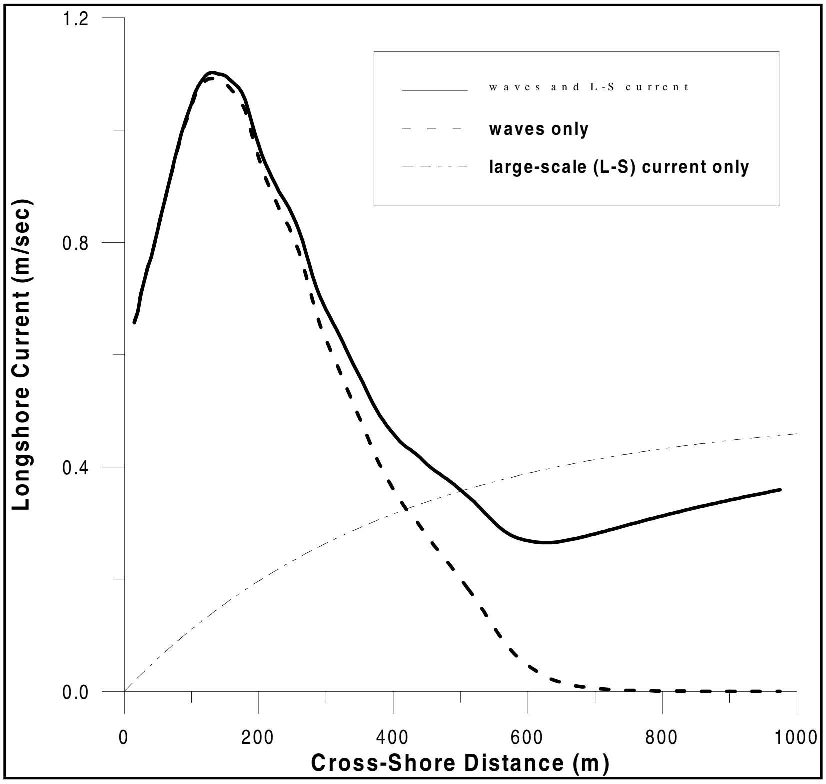

Figure 4. Simulation of the effect of a large-scale current on a wave-generated nearshore current

The example concerns wave transformation on flood and ebb currents. An inlet channel is simulated with a water depth of 4 m at the throat and linearly sloping offshore to a depth of 12 m (assumed boundary for this inlet). Waves are assumed to travel along the channel (0 incident wave angle), and the tidal current (flood or ebb) decreases linearly from the throat to the offshore end of the channel where it was set to 0 (at the 12-m water depth corresponding to $x = 0$ in Figure 5). The deepwater rms wave height was 1.0 m, and the mean wave period 8 sec (typical for Shinnecock Inlet). Standard parameter values were employed in the NMLong-CW simulations.

Figure 5 displays the results of the simulations for two different current speeds at the inlet throat for flood, ebb, and no-current cases. In the no-current case, a small increase in wave height is observed because of shoaling, whereas for the flood current the waves experience a reduction in height as they approach the inlet. The opposite trend occurs if the waves encounter an ebb flow and a pronounced wave height increase might take place. For example, in the case of an ebb current of 3.0 m/sec at the inlet throat, wave breaking occurs because of the limitation in wave steepness, causing a reduction in wave height, as seen in Figure 5 (note that the waves propagate along the x-axis to allow qualitative comparison with Figure 6). Also, for the larger ebb current, wave blocking is taking place before the waves reach the inlet throat. Figure 6 is a photograph taken from the east jetty at Shinnecock Inlet and shows wave breaking and blocking on an ebb current. Note that the waves cannot penetrate against the current, with turbulent water to the left (south) and calm water to the north, inside the inlet.

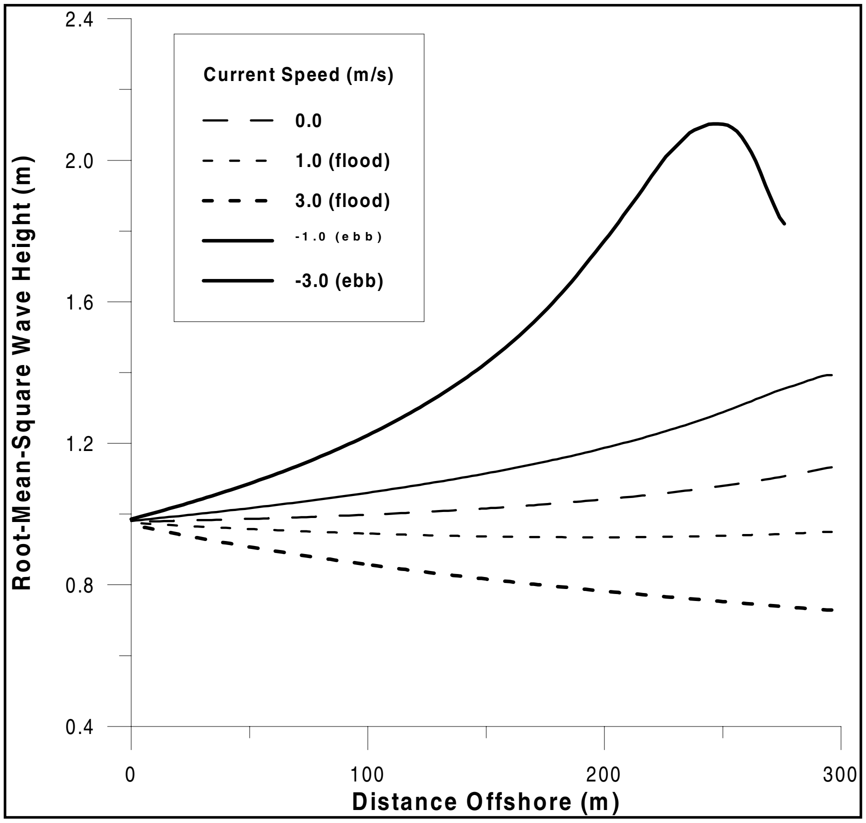

Figure 5. Calculated wave transformation on flood and ebb currents at an inlet

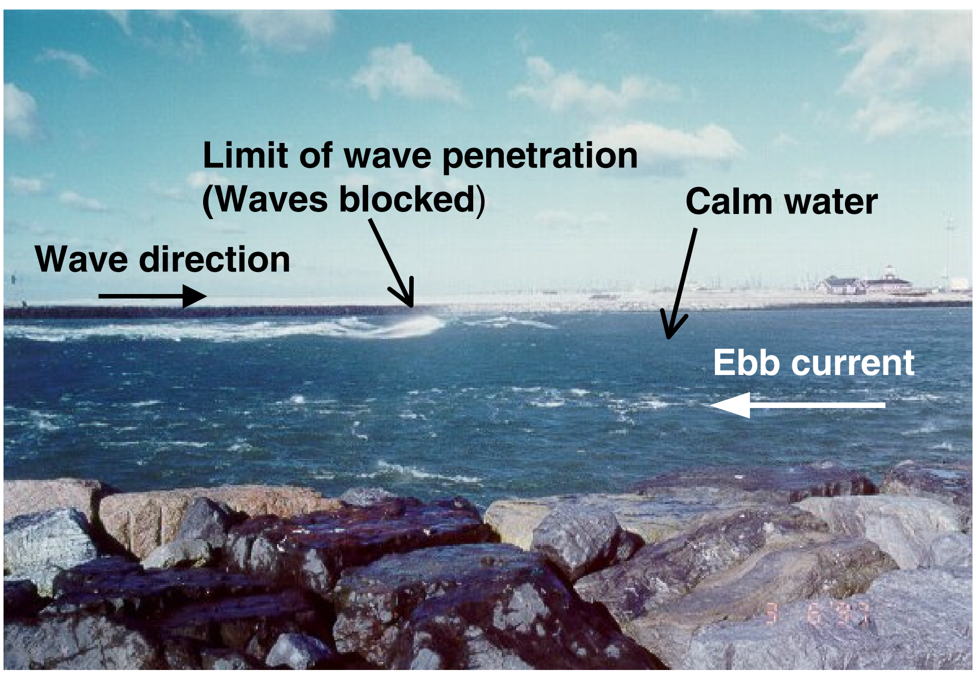

Figure 6. Wave breaking and blocking by an ebb current

By this example, it can be seen that the wave climate in an inlet channel can be investigated at reconnaissance level with NMLong-CW under the assumption of longshore uniformity. For example, under a given ebb current and offshore wave height and period, the increase in wave height and in wave steepness, defined as H/L, owing to the presence of the tidal current can be calculated. Steep waves pose a hazard to navigation if the wavelength approaches that of the vessel transiting the inlet.

FUTURE WORK: Research is underway in the CIRP to include longshore sediment transport in NMLong-WC. The model and interface will be revised to calculate longshore transport inside and seaward of the surf zone as associated with a current produced by waves, tide, and wind.

ADDITIONAL INFORMATION:

This CETN was written by Dr. Magnus Larson of the Department of Water Resources Engineering, Lund Institute of Technology, University of Lund, Sweden, and by Dr. Nicholas C. Kraus of the U.S. Army Engineer Research and Development Center (ERDC), Coastal and Hydraulics Laboratory. The work performed at the University of Lund was done under contract with the ERDC through the U.S. Army Engineer Research and Standardization Group-United Kingdom. Questions about this CETN can be addressed to Dr. Nicholas C. Kraus (601-634-2016, Fax 601-634-3080, e-mail: *KrausN@wes.army.mil*).

This CETN should be cited as follows:

> Larson, M., and Kraus, N.C., (2000). "Enhancements of the numerical model of the longshore current NMLONG to include interaction between currents and waves (NMLong-CW)," Coastal Engineering Technical Note CETN-IV-25, U.S. Army Engineer Research and Development Center, Vicksburg, MS, *http://chl.wes.army.mil/library/publications/cetn/*.

REFERENCES

Battjes, J., and Janssen, J.P.F.M. (1978). "Energy loss and setup due to breaking of random waves," *Proceedings 16th Coastal Engineering Conference*, ASCE, 569-587.

Dally, W.R., Dean, R.G., and Dalrymple, R.A. (1985). "Wave height variation across beaches of arbitrary profile," *Journal of Geophysical Research*, 90 (C6), 11, 917-11,927.

Dean, R.G. (1977). "Equilibrium beach profiles: U.S. Atlantic and Gulf coasts," Department of Civil Engineering, Ocean Engineering Report No. 12, University of Delaware, Newark, DE.

Jonsson, I.G., Skougaard, C., and Wang, J.D. (1970). "Interaction between waves and currents," *Proceedings 12th Coastal Engineering Conference*, ASCE, 489-507.

Jonsson, I.G. (1990). "Wave-current interactions," *The Sea*, B. Le Méhauté and D. Hanes, eds., John Wiley & Sons, New York, 65-120.

Kraus, N.C., and Larson, M. (1991). "NMLONG – Numerical model for simulating the longshore current. Report 1: Model development and tests," Technical Report DRP-91-1, U.S. Army Engineer Waterways Experiment Station, Coastal Engineering Research Center, Vicksburg, MS.

Larson, M., and Kraus, N.C. (1991). "Numerical model of longshore current for bar and trough beaches," *Journal of Waterway, Port, Coastal, and Ocean Engineering*, 117 (4), 326-347.

Nishimura, H. (1988). "Computation of nearshore current," *Nearshore Dynamics and Coastal Processes*, K. Horikawa, ed., University of Tokyo Press, Tokyo, Japan, 271-291.

Smith, J.M. (1997). "One-dimensional wave-current interaction," Coastal Engineering Technical Note CETN-IV-9, U.S. Army Engineer Waterways Experiment Station, Coastal Engineering Research Center, Vicksburg, MS.

Smith, J.M. (1999). "Wave breaking on an opposing current," Coastal Engineering Technical Note CETN-IV-17, U.S. Army Engineer Waterways Experiment Station, Coastal Engineering Research Center, Vicksburg, MS.

Smith, J.M., Resio, D.T., and Vincent, C.L. (1997). "Current-induced breaking at an inlet," *Proceedings Coastal Dynamics '97*, ASCE, 93-1002.

Smith, J.M., Seabergh, W.C., Harkins, G.S., and Briggs, M.J. (1998). "Wave breaking on a current at an idealized inlet; Coastal Inlets Research Program, Inlet Laboratory Investigations," Technical Report CHL-98-31, U.S. Army Engineer Waterways Experiment Station, Coastal Engineering Research Center, Vicksburg, MS.

WAMDI Group (1988). "The WAM Model – A third generation ocean wave prediction model," *Journal of Physical Oceanography*, December, 1775-1810.